JVI Accepted Manuscript Posted Online 1 March 2017
J. Virol. doi:10.1128/JVI.00003-17
Copyright © 2017 American Society for Microbiology. All Rights Reserved.

# Porcine Deltacoronavirus Nsp5 Antagonizes Type I Interferon Signaling by Cleaving STAT2

Xinyu Zhu[a,b], Dang Wang[a,b], Junwei Zhou[a,b], Ting Pan[a,b], Jiyao Chen[a,b], Yuting Yang[a,b], Mengting Lv[a,b], Xu Ye[a,b], Guiqing Peng [a,b], Liurong Fang[a,b#], Shaobo Xiao[a,b#]

[a]State Key Laboratory of Agricultural Microbiology, College of Veterinary Medicine, Huazhong Agricultural University, Wuhan 430070, China

[b]The Cooperative Innovation Center for Sustainable Pig Production, Wuhan 430070, China

[#]Corresponding authors. Laboratory of Animal Virology, College of Veterinary Medicine, Huazhong Agricultural University, 1 Shi-zi-shan Street, Wuhan 430070, Hubei, PR China. E-mails: fanglr@mail.hzau.edu.cn; vet@mail.hzau.edu.cn

**Running title***: PDCoV nsp5 cleaves STAT2*

**Abstract word count:** 239

**Main text word count:** 3636

JVI

## ABSTRACT

Porcine deltacoronavirus (PDCoV) is an emerging swine enteropathogenic coronavirus. The first outbreak of PDCoV was announced from the United States in 2014, followed by reports in Asia. The nonstructural protein nsp5 is a 3C-like protease of coronavirus and our previous study showed that PDCoV nsp5 inhibits type I interferon (IFN) production. In this study, we found that PDCoV nsp5 significantly inhibited IFN-stimulated response element (ISRE) promoter activity and transcription of IFN-stimulated genes (ISGs), suggesting that PDCoV nsp5 also suppresses IFN signaling. Detailed analysis showed that nsp5 cleaved signal transducer and activator of transcription 2 (STAT2), but not Janus kinase 1 (JAK1), tyrosine kinase 2 (TYK2), STAT1 and interferon regulatory factor 9 (IRF9), key molecules of the JAK-STAT pathway. STAT2 cleavage was dependent on the protease activity of nsp5. Interestingly, nsp5 cleaved STAT2 at two sites, glutamine (Q) 685 and Q758, and similar cleavage was observed in PDCoV-infected cells. As expected, cleaved STAT2 impaired the ability to induce ISGs, demonstrating that STAT2 cleavage is an important mechanism utilized by PDCoV nsp5 to antagonize IFN signaling. We also discussed the substrate selection and binding mode of PDCoV nsp5 by homologous modeling of PDCoV nsp5 with the two cleaved peptide substrates. Taken together, our study demonstrates that PDCoV nsp5 antagonizes type I IFN signaling by cleaving STAT2 and provides structural insights to comprehend the cleavage mechanism of PDCoV nsp5, revealing a potential new function for PDCoV nsp5 in type I IFN signaling.

## IMPORTANCE

The 3C-like protease encoded by nsp5 is a major protease of coronaviruses; thus it is an attractive target for development of anti-coronavirus drugs. Previous studies have revealed that the 3C-like protease of coronaviruses, including PDCoV and porcine epidemic diarrhea virus (PEDV), antagonizes type I IFN production by targeting NF-κB essential modulator (NEMO). Here, for the first time, we demonstrate that overexpression of PDCoV nsp5 also antagonizes IFN signaling by cleaving STAT2, an essential component of transcription factor complex ISGF3, and that PDCoV infection reduces the levels of STAT2, which may affect the innate immune response.

JVI

## INTRODUCTION

Porcine deltacoronavirus (PDCoV) is an emerging swine enteropathogenic coronavirus (CoV), which causes acute diarrhea, vomiting, and mortality in piglets (1-4). PDCoV was first found from pig feces in Hong Kong during molecular surveillance of CoVs in avian and mammalian species in 2012 (5). The first outbreak of PDCoV was announced in the United States in 2014 (6). To date, it has been detected in at least 20 states of the United States (3, 7, 8), as well as Canada, South Korea (9), China (10-12), Thailand (13), Lao People's Democratic Republic, and Vietnam (14), posing a significant threat to the swine industry and gaining considerable attention (13, 15, 16).

PDCoV is an enveloped, single-stranded positive-sense RNA virus and belongs to the genus *Deltacoronavirus* in the family *Coronaviridae* (5, 17). The PDCoV genome, approximately 25 kb in length, encodes four structural proteins, spike (S), envelope (E), membrane (M), and nucleocapsid (N), and three accessory proteins, NS6, NS7, and NS7a, interspersed within the structural genes at the 3′ end of the genome (5, 18, 19). Open reading frame (ORF)1a and ORF1b are located downstream from the 5′ untranslated region and encode two polyprotein precursors that are predicted to be processed into 15 mature nonstructural proteins (nsps) by the papain-like protease, nsp3 and the 3C-like protease, nsp5 (20, 21). Because of the essential function of nsp5 in viral replication, it has become an attractive target for the development of anti-CoV drugs (22, 23). Understanding in detail the function and structural characteristics of PDCoV nsp5 will aid in development of targeted therapies against CoV infection.

Interferon (IFN) and the IFN-induced cellular antiviral response are primary defense mechanisms against viral infection (24). Type I IFN binds to its surface receptor at two subunits, IFNAR1 and IFNAR2, and induces heterodimerization of the receptor subunits. Subsequently, Janus kinase 1 (JAK1) and tyrosine kinase 2 (TYK2) are activated and phosphorylate the cytoplasmic domains of IFNAR1 and IFNAR2 to establish docking sites for signal transducer and activator of transcription 1 (STAT1) and STAT2 (25, 26). STAT1 and STAT2 are then phosphorylated by JAK1 and TYK2, leading to heterodimer formation of phosphorylated STAT1 and phosphorylated STAT2 (26, 27). This complex interacts with IFN regulatory factor 9 (IRF9) to form IFN-stimulated gene factor 3 (ISGF3), which is transported into the nucleus and recognizes IFN-stimulated response elements (ISREs), enhancing the transcription of hundreds of IFN-stimulated genes (ISGs) (28, 29). As effective antiviral factors, ISGs directly lead to resistance to viral infection by targeting viral processes such as transcription and translation.

Given the importance of JAK-STAT pathway in the IFN signaling, it is not surprising that viruses have evolved mechanisms that target it to inhibit ISG production. Many studies have demonstrated that viral proteins, such as the NS5 protein of dengue virus (DENV), Zika virus (ZIKV), and the hepatitis C virus (HCV) core protein, target the JAK-STAT pathway by diverse mechanisms to negatively modulate IFN signaling (30-32). We previously demonstrated that PDCoV nsp5 antagonizes IFN-β production by cleaving NF-κB essential modulator (NEMO) (33).

However, whether nsp5 regulates IFN signaling remains unclear. In this study, we found that PDCoV nsp5 suppressed type I IFN signaling by cleaving STAT2, a key molecule in the JAK-STAT pathway, revealing a potential new function for PDCoV nsp5 in type I IFN signaling.

## RESULTS

**Identification of PDCoV nsp5 as an antagonist of type I IFN signaling.** Type I IFN signaling induces a potent antiviral state by enhancing the expression of hundreds of ISGs, which are critical for controlling viral infections (34). To assess the regulatory role of PDCoV nsp5 in type I IFN signaling, mRNA levels of ISG15, ISG54, ISG56, and OAS1 were evaluated under PDCoV nsp5 overexpression in human embryonic kidney cells (HEK-293T). As shown in Fig. 1A, ISG transcription induced by IFN-α was significantly inhibited by PDCoV nsp5 compared with the control group. Because of the existence of ISREs within ISG promoter regions, various concentrations of PDCoV nsp5 expression plasmid and ISRE-luciferase reporter plasmid were co-transfected into HEK-293T cells, porcine kidney cells (PK-15) or swine testicular cells (ST). The results showed that nsp5 strongly inhibited IFN-α-induced ISRE promoter activity in a dose-dependent manner in HEK-293T cells (Fig. 1B), PK-15 cells (Fig. 1C) and ST cells (Fig. 1D). These results confirm the antagonistic property of PDCoV nsp5 in type I IFN signaling.

**PDCoV nsp5-mediated inhibition of type I IFN signaling requires its protease**

JVI

**activity.** Because cysteine (Cys) and histidine (His) residues of CoV nsp5 form a catalytic dyad, any mutation in the catalytic site can disrupt its protease activity (22, 35, 36). Secondary structure alignment showed that residues His41 and Cys144 (numbering based on PDCoV nsp5) are highly conserved among the four genera of alpha-, beta-, gamma-, and delta-CoVs (Fig. 2A). We further created a homology model of PDCoV nsp5 based on the crystal structures of porcine epidemic diarrhea virus (PEDV) nsp5 (PDB identifier 4ZUH) using MODELLER 9.14 software and compared it with the three-dimensional (3D) structures of PEDV nsp5 (alpha-CoV), severe acute respiratory syndrome coronavirus (SARS-CoV) nsp5 (beta-CoV), and infectious bronchitis virus (IBV) nsp5 (gamma-CoV). As shown in Fig. 2B, the locations of the catalytic residues are also conserved in the 3D structures of PEDV nsp5, SARS-CoV nsp5, IBV nsp5, and PDCoV nsp5. Thus, two mutations, nsp5 H41A and nsp5 C144A, in the catalytic dyad were constructed. Compared with overexpression of wild-type PDCoV nsp5, repression of IFN-α-induced ISRE promoter activity was strongly relieved with overexpression of nsp5 H41A or nsp5 C144A (Fig. 2C). This finding suggests that the protease activity of PDCoV nsp5 is involved in antagonizing type I IFN signaling.

**PDCoV nsp5 antagonizes type I IFN signaling by targeting STAT2.** To determine the mechanism by which PDCoV nsp5 inhibits type I IFN signaling, the endogenous protein level and phosphorylation of JAK1, TYK2, STAT1, and STAT2 were examined in IFN-α-treated LLC-PK1 cells (porcine kidney cell line). As shown in Fig.

3A, the expression and phosphorylation of JAK1 and TYK2 were not affected by PDCoV nsp5. However, STAT2 phosphorylation was impaired by PDCoV nsp5 after IFN-α treatment and the expression of total STAT2 was reduced (Fig. 3B). Thus, we did not exclude the possibility that the weaker band of P-STAT2 in the presence of nsp5 is probably due to the reduced levels of total STAT2. In addition, a slight reduction in endogenous STAT1 expression was also observed (Fig. 3B).

As for the importance of PDCoV nsp5 protease activity in antagonizing type I IFN signaling, we considered whether PDCoV nsp5 cleaves specific molecules. Therefore, nsp5 was transfected into HEK-293T cells, along with JAK1, TYK2, STAT1, STAT2, or IRF9. No cleaved products were detected with JAK1, TYK2, STAT1, or IRF9 cotransfection. However, two faster migrating protein bands were observed by western blot analysis in cells cotransfected with STAT2 and PDCoV nsp5, indicating that PDCoV nsp5 mediates cleavage of STAT2 (Fig. 3C). Although nsp5 overexpression also slightly reduced the protein abundance of endogenous STAT1 (Fig. 3B), no cleavage product of Flag-STAT1 in nsp5-transfected cells was detected by an anti-Flag antibody (Fig. 3C). The nsp5-mediated reduction in endogenous STAT1 expression was not investigated further in this study.

**PDCoV nsp5 cleaves STAT2 through its protease activity.** To further confirm nsp5 cleavage of STAT2, HEK-293T cells were cotransfected with STAT2 and various concentrations of PDCoV nsp5. PDCoV nsp5 induced STAT2 cleavage in a dose-dependent manner (Fig. 4A). Additionally, STAT2 cleavage was not observed in

JVI

cells cotransfected with nsp5 H41A or nsp5 C144A (Fig. 4B). Furthermore, PDCoV nsp5-induced STAT2 cleavage was not affected by treatment with caspase inhibitor Z-VAD-FMK or proteasome inhibitor MG132, confirming this cleavage occurred independent of cellular caspases or the proteasome (Fig. 4C). Taken together, PDCoV nsp5 cleavage of STAT2 appears to occur through its protease activity.

To further evaluate the expression of endogenous STAT2 in PDCoV infection, the mRNA and protein levels of endogenous STAT2 were determined in PDCoV-infected LLC-PK1 cells. Although STAT2 mRNA in PDCoV-infected cells slightly increased compared with the mock-infected group (Fig. 4D), endogenous STAT2 protein was clearly decreased with PDCoV infection (Fig. 4E). Remarkably, the cleavage of endogenous STAT2 was also detected in PDCoV-infected cells (Fig. 4E), revealing the biological effect of this cleavage in virus infection.

**PDCoV nsp5 cleaves STAT2 at residues Q685 and Q758.** To further identify the cleavage sites of STAT2 by PDCoV nsp5, substrate specificity of PDCoV nsp5 in viral polyprotein itself was analyzed. As shown in Fig. 5A, a preference for substrate cleavage by PDCoV nsp5 was Q residue at the P1 position, which is common among other CoV subfamilies (1, 37). Because the cleavage of N-terminally Flag-tagged STAT2 by PDCoV nsp5 yielded a slightly longer than 70 kDa in Fig. 3C detected by anti-Flag antibody, a cluster of potential nsp5 cleavage sites were suggested to be in the carboxyl-terminal region of STAT2. Considering the molecule weight of cleavage products and the conserved Q residue at the P1 position in substrate recognition by

JVI

coronavirus nsp5, the deletion mutants, STAT2 (1–637 aa), STAT2 (1–719 aa), and STAT2 (1–758 aa) were generated. The two cleavage products of STAT2 were longer in size than STAT2 (1–637 aa), indicating that the recognized Q residue of the P1 position should be located at the C-terminal region (residues 637–864 aa) of STAT2 (Fig. 5B). Eight Q residues (637–864 aa region) were subsequently changed to alanine (Fig. 5C) and transfected into HEK-293T cells along with PDCoV nsp5. The two cleavage products separately disappeared under the expression of Q685A or Q758A (Fig. 5D), while other mutants were cleaved into two new products as expected by PDCoV nsp5, demonstrating the two potential cleaved positions to be Q685 and Q758. To further confirm these cleaved residues, a double mutant (STAT2-Q685A-Q758A) was constructed and cotransfected into HEK-293T cells with PDCoV nsp5. The results showed that STAT2-Q685A-Q758A was resistant to cleavage, confirming Q685 and Q758 to be the two P1 position residues recognized by PDCoV nsp5 for cleavage of STAT2 (Fig. 5E).

**PDCoV nsp5-mediated cleavage impairs STAT2's ability to induce ISGs.** To assess the effect of STAT2 cleavage by PDCoV nsp5 in type I IFN signaling, several deletion mutations encoding STAT2 cleavage products, including STAT2 (1–685 aa), STAT2 (1–758 aa), STAT2 (686–864 aa), STAT2 (759–864 aa), and STAT2 (686–758 aa), were generated based on the identified cleaved residues. Full-length STAT2, individual deletion mutants, or mixed deletion mutants were cotransfected with STAT1 and IRF9, along with ISRE-luciferase reporter plasmid and pRL-TK.

JVI

Compared with full-length STAT2, the luciferase activity of ISRE-Luc significantly decreased under the expression of any cleaved fragments (Fig. 6A). The mRNA levels of ISGs, such as ISG15 (Fig. 6B), ISG54 (Fig. 6C) and OAS1 (Fig. 6D), were also not sufficiently induced by the cleaved STAT2 fragments. These results reveal that STAT2 cleavage induced by PDCoV nsp5 impairs the ability of STAT2 to activate type I IFN signaling.

## DISCUSSION

As a powerful antiviral response, type I IFN signaling can control viral infections through activation of the transcription factor complex ISGF3, resulting in increased transcription of hundreds of ISGs that help to generate an antiviral state. However, viruses have developed diverse strategies to inhibit type I IFN signaling. STAT2, an essential component of ISGF3 activity, is a common target hijacked by viral proteins. For example, the NS5 protein of flaviviruses, such as DENV and ZIKV, target STAT2 for degradation (30, 31). The HCV core protein was also reported to interact with STAT2 to disturb the function of ISGF3 complex (32). Phosphorylation of STAT2 was inhibited by C protein of Sendai virus, and yellow fever virus NS5 protein could prevent STAT2 binding to ISRE promoter (38, 39). However, the relationship between proteins encoded by CoVs and IFN signaling inhibition remains largely unclear. Limited research has shown that SARS-CoV nsp1 and ORF6 target STAT1 through inhibition of its phosphorylation or nuclear translocation, respectively (40, 41). SARS-CoV PLpro can disrupt the interaction between ERK1 and STAT1 to

JVI

antagonize type I IFN signaling (42). Here, we established that PDCoV nsp5, a 3C-like protease, targeted STAT2 for cleavage. Furthermore, our study demonstrated that PDCoV nsp5 disrupted type I IFN signaling by cleaving STAT2, which was contributed by PDCoV nsp5 protease activity, independent of the ubiquitin proteasome pathway or apoptotic pathway. Importantly, endogenous STAT2 in PDCoV-infected cells was cleaved, which is consistent with the effect of nsp5 overexpression. These results confirm the antagonistic property of PDCoV nsp5 in type I IFN signaling, which may affect the IFN response after PDCoV infection.

We previously demonstrated that PDCoV nsp5 cleaves NEMO, a vital adaptor of the IKK complex, to reduce type I IFN production (33). The role of PDCoV nsp5 in both IFN production and IFN signaling blockage suggests that PDCoV nsp5 limits the IFN-induced antiviral state in infected cells and contributes to rapid spread of PDCoV from an infected cell to neighboring cells. However, the relative impact of either NEMO or STAT2 in cells with PDCoV infection is unclear. Based on the identified residues of STAT2 and NEMO cleaved by PDCoV nsp5, to establish a cell line that expresses forms of NEMO and STAT2 with mutated cleavage sites will be helpful to evaluate the functional significance of potential cleavage of STAT2 or NEMO during PDCoV infection. In addition, NEMO and STAT2 are vital molecules for IFN production and IFN signaling, respectively. Previous studies have demonstrated that NEMO can be cleaved by the 3C or 3C-like proteases of PEDV, Hepatitis A virus (HAV), Food-and-mouth disease virus (FMDV), and Porcine reproductive and respiratory syndrome virus (PRRSV) (43-46). To investigate

JVI

whether STAT2 cleavage is a shared attribute among 3C-like proteases of different coronaviruses, we analyzed the nsp5 of two porcine coronaviruses, PEDV and transmissible gastroenteritis virus (TGEV), and five human coronaviruses (HCoVs) including SARS-CoV, Middle East respiratory syndrome virus (MERS-CoV), HCoV-229E, HCoV-OC43, and HCoV-NL63. We found that porcine STAT2 could not be cleaved by the nsp5 of PEDV and TGEV, and human STAT2 could not be cleaved by the nsp5 of all tested human coronaviruses (data not shown). However, whether cleavage of STAT2 is unique to PDCoV nsp5 requires further evidence in other coronaviruses.

It is well known that STAT2 exhibits several functionally conserved regions, such as the critical tyrosine residue (Y690), which is phosphorylated to mediate STAT heterodimerization and transcription activation, and the transcriptional activation domain (TAD) at the C-terminal end, which is responsible for transcriptional activity after the ISGF3 complex binds to DNA (47-49). Our present study identified that PDCoV nsp5 cleaves STAT2 residues Q685 and Q758. It is considered that cleavage of Q685 by PDCoV nsp5 could disrupt the function of Y690 and inhibit STAT2 activation. This finding also helps explain impaired tyrosine phosphorylation of STAT2 under PDCoV nsp5 overexpression upon IFN-α stimulation. The second cleavage of Q758, which is located in the TAD of STAT2, is inevitable to further disrupt the TAD, which helps to recruit other transcription co-factors. This may help explain why other cleavage products or the mixture of cleaved products of STAT2 along with STAT1 and IRF9 failed to efficiently activate ISRE promoter activity.

Taken together, cleavage at Q685 and Q758 by PDCoV nsp5 damaged the structural and functional integrity of STAT2, and affected subsequent STAT2 phosphorylation and ISGs induction.

According to previous studies on CoVs, the general substrate recognized by CoV nsp5 was determined to be mainly the P1, P2, and P1′ residues (50, 51). As shown by the analysis of PDCoV nsp5 substrate specificity (Fig. 5A), the P1 residue was a conserved Q residue and the P2 residue was primarily a leucine (L), which has a large side chain. Additionally, small residues generally occupy the P1′ position. The peptides EKANLQ$_{685}$↓ERKKYL and LEPMLQ$_{758}$↓STLEPV (P6 to P6′; numbering based on STAT2) recognized by PDCoV nsp5 at the P1 and P2 positions are generally conserved substrates for all CoVs. However, glutamic acid (E) at the P1′ position, which shared a large negatively-charged side chain responsible for Q685 cleavage, was unusual. Therefore, the homology model for PDCoV nsp5 in complex with these two peptide substrates was constructed based on the structure of PEDV nsp5 (PDB identifier 4ZUH) to further investigate the changes at the P1′ position between the two substrates of STAT2. The PDCoV nsp5 S1′ subsite is composed of S25, A26, L27, C38, P39, H41, and V42 (Fig. 7A and 7B). The model showed that the long side chain of P1′-E fit comfortably in the pocket. Detailed molecular interactions between the two substrates and PDCoV nsp5 showed that the conserved Q at the P1 position was stabilized by two hydrogen bonds with H162 and E165, and the main chain of P2′-residue formed two hydrogen bonds with the main chain of A26 (Fig. 7C and 7D). Previous studies showed that PEDV nsp5 tolerates the positively-charged side chain of arginine (R) of PEDV N protein and a larger hydrophobic residue valine (V) of NEMO at the P1′ position for cleavage (36, 43, 52). Our analysis revealed that the S1′ subsite of PDCoV nsp5 demonstrates flexibility to tolerate residues with a large negatively-charged side chain instead of small aliphatic residues, suggesting a broader selection in PDCoV nsp5 substrate recognition. Thus, the complete crystal structure of nsp5 and the cleaved peptide substrates of STAT2 could provide more direct evidence and detailed information of molecular interactions between the substrate and nsp5, aiding in the design of targeted drugs against PDCoV nsp5.

Similar to PDCoV, PEDV is a swine enteropathogenic CoV. Of 23 PEDV-encoded proteins, at least 10 proteins have been identified as IFN antagonists (53). The mechanisms utilized by PEDV nsp1, nsp5, PLP2, and N protein to antagonize type I IFN production have been elucidated (43, 53-55). As a newly emerging enteric CoV, the molecular mechanism by which PDCoV regulates IFN activity remains largely unknown. To date, only PDCoV nsp5 has been identified as an antagonist of both type I IFN production (33) and type I IFN signaling (present study). The further identification of PDCoV-encoded IFN antagonists and understanding of the interaction between PDCoV and the IFN signaling pathway will help to develop novel therapeutic targets and more effective vaccines.

## MATERIALS AND METHODS

**Cells and viruses**. HEK-293T and PK-15 cells, obtained from the China Center for Type Culture Collection, were cultured at 37°C in 5% $CO_2$ in Dulbecco's Modified

JVI

Eagle's medium (Invitrogen, USA) supplemented with 10% fetal bovine serum. LLC-PK1 cells for PDCoV infection were acquired from the ATCC (ATCC number CL-101) and cultured at the same condition described above. PDCoV strain CHN-HN-2014 (GenBank accession number KT336560) was isolated from a piglet with severe diarrhea in China in 2014 (56).

**Plasmids and luciferase reporter assay.** Nsp5 gene of PDCoV strain CHN-HN-2014 was amplified and cloned into pCAGGS-HA-C with a C-terminal HA tag. PDCoV nsp5 mutants were also constructed in the pCAGGS-HA-C background. Porcine STAT1, STAT2, IRF9, JAK1, and TYK2 were cloned into pCAGGS-Flag with an N-terminal Flag tag. All STAT2 substitution mutants were constructed in the pCAGGS-Flag background by overlap extension PCR using specific mutagenic primers (available upon request). STAT2 deletion mutants were also cloned into pCAGGS-Flag. All constructed plasmids were confirmed by sequencing.

The luciferase reporter plasmid ISRE-Luc used in this study has been previously described (57). For luciferase reporter assays, HEK-293T cells were transfected with reporter plasmid ISRE-Luc and pRL-TK. Twenty-four hours after transfection, the cells were stimulated with IFN-α (Catalog no. 11101-2, PBL Assay Science) for 12 h at a final concentration of 1,000 U/ml. The lysed cells were prepared and the luciferase reporter assay system (Promega, Madison, WI) was utilized to determine the luciferase activities of lysed cells. The activities were normalized to that of pRL-TK (Promega).

**RNA extraction and quantitative real-time PCR**. To determine the effect of PDCoV nsp5 on the expression of ISGs, including ISG15, ISG54, ISG56, and OAS1, HEK-293T cells in 24-well plates were transfected with 1 µg of empty vector or nsp5 expression plasmid. After 24 h, the cells were treated with IFN-α (1,000 U/ml) for 12 h. To evaluate the ability of the cleavage products of STAT2 to induce ISGs, full-length STAT2 or its deletion mutants were cotransfected with STAT1 and IRF9 into PK-15 cells for 32 h. Total RNA was extracted from transfected cells with TRIzol reagent (Invitrogen). RNA was then reverse transcribed into cDNA by avian myeloblastosis virus reverse transcriptase (TaKaRa, Japan). Quantitative real-time PCR (qPCR) experiments were performed in triplicate. mRNA expression levels were normalized to that of glyceraldehyde-3-phosphate dehydrogenase (GAPDH). All qPCR primers used in this study are listed in Table 1.

**Western blot analyses.** Cells were cultured in 60-mm dishes and harvested with lysis buffer (Beyotime, China). The samples were then resolved by SDS-PAGE and transferred to polyvinylidene difluoride membranes (Millipore, USA) to determine protein expression. Cells were also treated with a broad caspase inhibitor (Z-VAD-FMK; Beyotime, China) or a proteasome inhibitor (MG132; Beyotime, China) at a final concentration of 20 µM. The overexpression of JAK1, TYK2, IRF9, STAT1, STAT2, and STAT2 mutants was evaluated using an anti-Flag antibody (Macgene, China). An anti-HA antibody (MBL, Japan) was used to analyze the expression of PDCoV nsp5. STAT1 polyclonal antibody (Santa Cruz, USA), STAT2

JVI

antibody (ABclonal, China), JAK1 antibody (Cell Signaling Technology, USA), and TYK2 antibody (Cell Signaling Technology, USA) were utilized to detect each respective endogenous protein. Phospho-STAT1 antibody (Cell Signaling Technology, USA), Phospho-STAT2 antibody (ABclonal, China), Phospho-JAK1 antibody (Cell Signaling Technology, USA), and Phospho-TYK2 antibody (Cell Signaling Technology, USA) were utilized to identify the phosphorylated form of each respective endogenous protein.

**Homology modeling.** A BLASTP search of PDCoV nsp5 sequence against the Protein Data Bank (PDB) library revealed PEDV nsp5 (PDB identifier 4ZUH) to be a close homolog. Thus, the homology model of PDCoV nsp5 was generated based on the crystal structures of PEDV nsp5 using MODELLER 9.14 software (58). The distribution of hydrophobic and hydrophilic interactions between the substrates and protease was created by the LigPlot+ program.

**Statistical analysis.** All experiments were performed in triplicate. Significant differences were determined using Student's *t* test. P values <0.05 were considered statistically significant.

## ACKNOWLEDGEMENT

This work was supported by the National Key R&D Plan of China (2016YFD0500103), the Key Technology R&D Programme of China

JVI

(2015BAD12B02), the National Natural Science Foundation of China (31672566), and the Natural Science Foundation of Hubei Province (2014CFA009).

## REFERENCE

1. **Chen Q, Gauger P, Stafne M, Thomas J, Arruda P, Burrough E, Madson D, Brodie J, Magstadt D, Derscheid R, Welch M, Zhang J.** 2015. Pathogenicity and pathogenesis of a United States porcine deltacoronavirus cell culture isolate in 5-day-old neonatal piglets. Virology **482:**51-59.
2. **Jung K, Hu H, Eyerly B, Lu Z, Chepngeno J, Saif LJ.** 2015. Pathogenicity of 2 porcine deltacoronavirus strains in gnotobiotic pigs. Emerg Infect Dis **21:**650-654.
3. **Ma Y, Zhang Y, Liang X, Lou F, Oglesbee M, Krakowka S, Li J.** 2015. Origin, evolution, and virulence of porcine deltacoronaviruses in the United States. MBio **6:**e00064.
4. **Hu H, Jung K, Vlasova AN, Saif LJ.** 2016. Experimental infection of gnotobiotic pigs with the cell-culture-adapted porcine deltacoronavirus strain OH-FD22. Arch Virol **161:**3421-3434.
5. **Woo PC, Lau SK, Lam CS, Lau CC, Tsang AK, Lau JH, Bai R, Teng JL, Tsang CC, Wang M, Zheng BJ, Chan KH, Yuen KY.** 2012. Discovery of seven novel Mammalian and avian coronaviruses in the genus deltacoronavirus supports bat coronaviruses as the gene source of alphacoronavirus and betacoronavirus and avian coronaviruses as the gene source of gammacoronavirus and deltacoronavirus. J Virol **86:**3995-4008.
6. **Wang L, Byrum B, Zhang Y.** 2014. Detection and genetic characterization of deltacoronavirus in pigs, Ohio, USA, 2014. Emerg Infect Dis **20:**1227-1230.
7. **Wang L, Byrum B, Zhang Y.** 2014. Porcine coronavirus HKU15 detected in 9 US states, 2014. Emerg Infect Dis **20:**1594-1595.
8. **Homwong N, Jarvis MC, Lam HC, Diaz A, Rovira A, Nelson M, Marthaler D.** 2016. Characterization and evolution of porcine deltacoronavirus in the United States. Prev Vet Med **123:**168-174.
9. **Lee JH, Chung HC, Nguyen VG, Moon HJ, Kim HK, Park SJ, Lee CH, Lee GE, Park BK.** 2016. Detection and Phylogenetic Analysis of Porcine Deltacoronavirus in Korean Swine Farms, 2015. Transbound Emerg Dis **63:**248-252.
10. **Dong N, Fang L, Zeng S, Sun Q, Chen H, Xiao S.** 2015. Porcine Deltacoronavirus in Mainland China. Emerg Infect Dis **21:**2254-2255.
11. **Song D, Zhou X, Peng Q, Chen Y, Zhang F, Huang T, Zhang T, Li A, Huang D, Wu Q, He H, Tang Y.** 2015. Newly Emerged Porcine Deltacoronavirus Associated With Diarrhoea in Swine in China: Identification, Prevalence and Full-Length Genome Sequence Analysis. Transbound Emerg Dis **62:**575-580.
12. **Wang YW, Yue H, Fang W, Huang YW.** 2015. Complete Genome Sequence of Porcine Deltacoronavirus Strain CH/Sichuan/S27/2012 from Mainland China. Genome Announc **3**:e00945-15.
13. **Janetanakit T, Lumyai M, Bunpapong N, Boonyapisitsopa S, Chaiyawong S, Nonthabenjawan N, Kesdaengsakonwut S, Amonsin A.** 2016. Porcine Deltacoronavirus,

Thailand, 2015. Emerg Infect Dis **22:**757-759.

14. **Saeng-Chuto K, Lorsirigool A, Temeeyasen G, Vui DT, Stott CJ, Madapong A, Tripipat T, Wegner M, Intrakamhaeng M, Chongcharoen W, Tantituvanont A, Kaewprommal P, Piriyapongsa J, Nilubol D.** 2017. Different Lineage of Porcine Deltacoronavirus in Thailand, Vietnam and Lao PDR in 2015. Transbound Emerg Dis **64**:3-10.
15. **Zhang J.** 2016. Porcine deltacoronavirus: Overview of infection dynamics, diagnostic methods, prevalence and genetic evolution. Virus Res **226:**71-84.
16. **Jung K, Hu H, Saif LJ.** 2016. Porcine deltacoronavirus infection: Etiology, cell culture for virus isolation and propagation, molecular epidemiology and pathogenesis. Virus Res **226:**50-59.
17. **Woo PC, Lau SK, Huang Y, Yuen KY.** 2009. Coronavirus diversity, phylogeny and interspecies jumping. Exp Biol Med (Maywood) **234:**1117-1127.
18. **Fang P, Fang L, Hong Y, Liu X, Dong N, Ma P, Bi J, Wang D, Xiao S.** 2016. Discovery of a novel accessory protein NS7a encoded by porcine deltacoronavirus. J Gen Virol doi:10.1099/jgv.0.000690.
19. **Fang P, Fang L, Liu X, Hong Y, Wang Y, Dong N, Ma P, Bi J, Wang D, Xiao S.** 2016. Identification and subcellular localization of porcine deltacoronavirus accessory protein NS6. Virology **499:**170-177.
20. **Li G, Chen Q, Harmon KM, Yoon KJ, Schwartz KJ, Hoogland MJ, Gauger PC, Main RG, Zhang J.** 2014. Full-Length Genome Sequence of Porcine Deltacoronavirus Strain USA/IA/2014/8734. Genome Announc **2**:e00278-14.
21. **Chen F, Zhu Y, Wu M, Ku X, Yao L, He Q.** 2015. Full-Length Genome Characterization of Chinese Porcine Deltacoronavirus Strain CH/SXD1/2015. Genome Announc **3**:e01284-15.
22. **Anand K, Ziebuhr J, Wadhwani P, Mesters JR, Hilgenfeld R.** 2003. Coronavirus main proteinase (3CLpro) structure: basis for design of anti-SARS drugs. Science **300:**1763-1767.
23. **Thiel V, Ivanov KA, Putics A, Hertzig T, Schelle B, Bayer S, Weissbrich B, Snijder EJ, Rabenau H, Doerr HW, Gorbalenya AE, Ziebuhr J.** 2003. Mechanisms and enzymes involved in SARS coronavirus genome expression. J Gen Virol **84:**2305-2315.
24. **Randall RE, Goodbourn S.** 2008. Interferons and viruses: an interplay between induction, signalling, antiviral responses and virus countermeasures. J Gen Virol **89:**1-47.
25. **Sheppard P, Kindsvogel W, Xu W, Henderson K, Schlutsmeyer S, Whitmore TE, Kuestner R, Garrigues U, Birks C, Roraback J, Ostrander C, Dong D, Shin J, Presnell S, Fox B, Haldeman B, Cooper E, Taft D, Gilbert T, Grant FJ, Tackett M, Krivan W, McKnight G, Clegg C, Foster D, Klucher KM.** 2003. IL-28, IL-29 and their class II cytokine receptor IL-28R. Nat Immunol **4:**63-68.
26. **Ihle JN.** 1995. The Janus protein tyrosine kinase family and its role in cytokine signaling. Adv Immunol **60:**1-35.
27. **Darnell JE, Jr., Kerr IM, Stark GR.** 1994. Jak-STAT pathways and transcriptional activation in response to IFNs and other extracellular signaling proteins. Science **264:**1415-1421.
28. **Qureshi SA, Salditt-Georgieff M, Darnell JE, Jr.** 1995. Tyrosine-phosphorylated Stat1 and Stat2 plus a 48-kDa protein all contact DNA in forming interferon-stimulated-gene factor 3. Proc Natl Acad Sci U S A **92:**3829-3833.
29. **Stark GR, Kerr IM, Williams BR, Silverman RH, Schreiber RD.** 1998. How cells respond to interferons. Annu Rev Biochem **67:**227-264.

JVI

30. **Grant A, Ponia SS, Tripathi S, Balasubramaniam V, Miorin L, Sourisseau M, Schwarz MC, Sanchez-Seco MP, Evans MJ, Best SM, Garcia-Sastre A.** 2016. Zika Virus Targets Human STAT2 to Inhibit Type I Interferon Signaling. Cell Host Microbe **19:**882-890.

31. **Ashour J, Laurent-Rolle M, Shi PY, Garcia-Sastre A.** 2009. NS5 of dengue virus mediates STAT2 binding and degradation. J Virol **83:**5408-5418.

32. **Lin W, Kim SS, Yeung E, Kamegaya Y, Blackard JT, Kim KA, Holtzman MJ, Chung RT.** 2006. Hepatitis C virus core protein blocks interferon signaling by interaction with the STAT1 SH2 domain. J Virol **80:**9226-9235.

33. **Zhu X, Fang L, Wang D, Yang Y, Chen J, Ye X, Foda MF, Xiao S.** 2017. Porcine deltacoronavirus nsp5 inhibits interferon-beta production through the cleavage of NEMO. Virology **502:**33-38.

34. **Takaoka A, Yanai H.** 2006. Interferon signalling network in innate defence. Cell Microbiol **8:**907-922.

35. **Hsu MF, Kuo CJ, Chang KT, Chang HC, Chou CC, Ko TP, Shr HL, Chang GG, Wang AH, Liang PH.** 2005. Mechanism of the maturation process of SARS-CoV 3CL protease. J Biol Chem **280:**31257-31266.

36. **Ye G, Deng F, Shen Z, Luo R, Zhao L, Xiao S, Fu ZF, Peng G.** 2016. Structural basis for the dimerization and substrate recognition specificity of porcine epidemic diarrhea virus 3C-like protease. Virology **494:**225-235.

37. **Chuck CP, Chong LT, Chen C, Chow HF, Wan DC, Wong KB.** 2010. Profiling of substrate specificity of SARS-CoV 3CL. PLoS One **5:**e13197.

38. **Gotoh B, Takeuchi K, Komatsu T, Yokoo J.** 2003. The STAT2 activation process is a crucial target of Sendai virus C protein for the blockade of alpha interferon signaling. J Virol **77:**3360-3370.

39. **Laurent-Rolle M, Morrison J, Rajsbaum R, Macleod JM, Pisanelli G, Pham A, Ayllon J, Miorin L, Martinez-Romero C, tenOever BR, Garcia-Sastre A.** 2014. The interferon signaling antagonist function of yellow fever virus NS5 protein is activated by type I interferon. Cell Host Microbe **16:**314-327.

40. **Wathelet MG, Orr M, Frieman MB, Baric RS.** 2007. Severe acute respiratory syndrome coronavirus evades antiviral signaling: role of nsp1 and rational design of an attenuated strain. J Virol **81:**11620-11633.

41. **Frieman M, Yount B, Heise M, Kopecky-Bromberg SA, Palese P, Baric RS.** 2007. Severe acute respiratory syndrome coronavirus ORF6 antagonizes STAT1 function by sequestering nuclear import factors on the rough endoplasmic reticulum/Golgi membrane. J Virol **81:**9812-9824.

42. **Li SW, Lai CC, Ping JF, Tsai FJ, Wan L, Lin YJ, Kung SH, Lin CW.** 2011. Severe acute respiratory syndrome coronavirus papain-like protease suppressed alpha interferon-induced responses through downregulation of extracellular signal-regulated kinase 1-mediated signalling pathways. J Gen Virol **92:**1127-1140.

43. **Wang D, Fang L, Shi Y, Zhang H, Gao L, Peng G, Chen H, Li K, Xiao S.** 2016. Porcine Epidemic Diarrhea Virus 3C-Like Protease Regulates Its Interferon Antagonism by Cleaving NEMO. J Virol **90:**2090-2101.

44. **Wang D, Fang L, Wei D, Zhang H, Luo R, Chen H, Li K, Xiao S.** 2014. Hepatitis A virus 3C protease cleaves NEMO to impair induction of beta interferon. J Virol **88**:10252-10258.

45. **Wang D, Fang L, Li K, Zhong H, Fan J, Ouyang C, Zhang H, Duan E, Luo R, Zhang Z, Liu X, Chen H, Xiao S.** 2012. Foot-and-mouth disease virus 3C protease cleaves NEMO to impair innate immune signaling. J Virol **86**: 9311-9322.

46. **Huang C, Zhang Q, Guo X, Yu Z, Xu A, Tang J, Feng W.** 2014. Porcine reproductive and respiratory syndrome virus nonstructural protein 4 antagonizes beta interferon expression by targeting the NF-κB essential modulator. J Virol **88**:10934-10945.

47. **Bhattacharya S, Eckner R, Grossman S, Oldread E, Arany Z, D'Andrea A, Livingston DM.** 1996. Cooperation of Stat2 and p300/CBP in signalling induced by interferon-alpha. Nature **383:**344-347.

48. **Qureshi SA, Leung S, Kerr IM, Stark GR, Darnell JE Jr.** 1996. Function of Stat2 protein in transcriptional activation by alpha interferon. Mol Cell Biol **16:**288-293.

49. **Schindler C, Shuai K, Prezioso VR, Darnell JE Jr.** 1992. Interferon-dependent tyrosine phosphorylation of a latent cytoplasmic transcription factor. Science **257:**809-813.

50. **Ziebuhr J, Snijder EJ, Gorbalenya AE.** 2000. Virus-encoded proteinases and proteolytic processing in the Nidovirales. J Gen Virol **81:**853-879.

51. **Hsu WC, Chang HC, Chou CY, Tsai PJ, Lin PI, Chang GG.** 2005. Critical assessment of important regions in the subunit association and catalytic action of the severe acute respiratory syndrome coronavirus main protease. J Biol Chem **280:**22741-22748.

52. **Jaru-Ampornpan P, Jengarn J, Wanitchang A, Jongkaewwattana A.** 2017. Porcine epidemic diarrhea virus (PEDV) 3C-Like protease-mediated nucleocapsid processing: A possible link to viral cell-culture adaptability. J Virol **91:**e01660-16.

53. **Zhang Q, Shi K, Yoo D.** 2016. Suppression of type I interferon production by porcine epidemic diarrhea virus and degradation of CREB-binding protein by nsp1. Virology **489:**252-268.

54. **Ding Z, Fang L, Jing H, Zeng S, Wang D, Liu L, Zhang H, Luo R, Chen H, Xiao S.** 2014. Porcine epidemic diarrhea virus nucleocapsid protein antagonizes beta interferon production by sequestering the interaction between IRF3 and TBK1. J Virol **88:**8936-8945.

55. **Xing Y, Chen J, Tu J, Zhang B, Chen X, Shi H, Baker SC, Feng L, Chen Z.** 2013. The papain-like protease of porcine epidemic diarrhea virus negatively regulates type I interferon pathway by acting as a viral deubiquitinase. J Gen Virol **94:**1554-1567.

56. **Dong N, Fang L, Yang H, Liu H, Du T, Fang P, Wang D, Chen H, Xiao S.** 2016. Isolation, genomic characterization, and pathogenicity of a Chinese porcine deltacoronavirus strain CHN-HN-2014. Vet Microbiol **196:**98-106.

57. **Zhong H, Wang D, Fang L, Zhang H, Luo R, Shang M, Ouyang C, Ouyang H, Chen H, Xiao S.** 2013. Ubiquitin-specific proteases 25 negatively regulates virus-induced type I interferon signaling. PLoS One **8:**e80976.

58. **Sali A, Blundell TL.** 1993. Comparative protein modelling by satisfaction of spatial restraints. J Mol Biol **234:**779-815.

JVI

## FIGURE LEGENDS

**FIG 1. PDCoV nsp5 antagonizes type I IFN signaling. (A)** HEK-293T cells cultured in 24-well plates were transfected with PDCoV nsp5 expression plasmid or vector. After 24 h, cells were treated with 1,000 U/ml of IFN-α for 8 h and analyzed by qPCR. **(B, C and D)** HEK-293T cells (B), PK-15 cells (C) or ST cells (D) cultured in 24-well plates were transfected with various concentrations of PDCoV nsp5 expression plasmid along with ISRE-Luc plasmid and pRL-TK plasmid. After 24 h, cells were treated with 1,000 U/ml of IFN-α for 12 h, followed by luciferase assays.

**FIG 2. PDCoV nsp5-mediated inhibition of type I IFN signaling requires its protease activity. (A)** Sequence alignment of nsp5 for the four genera of CoVs. Delta-CoVs were represented by PDCoV (accession number ALS54085.1) and HUK13 (accession number YP_002308505.1); alpha-CoVs were represented by PEDV (accession number NC_004004) and NL63 (accession number AFV53147.1); beta-CoVs were represented by SARS-CoV (accession number NP_828850.1) and MHV (accession number NP_068668.2); and gamma-CoVs were represented by IBV (accession number NP_740623.1) and TCoV (accession number YP_001941178.1). Secondary structures of CoV nsp5s were analyzed using the ESPript website (http://espript.ibcp.fr/ESPript/ESPript/index.php). **(B)** Structural alignment of the conserved residues His41 and Cys144 in CoV nsp5s. The homology model of PDCoV nsp5 was generated based on the crystal structures of PEDV nsp5 by MODELLER 9.14 software. The 3D structures of PEDV nsp5 (PDB identifier 4ZUH), SARS-CoV

JVI

nsp5 (PDB identifier 2Q6G), and IBV nsp5 (PDB identifier 2Q6D) were obtained from the Protein Data Bank. Red arrows indicate conserved enzymatic proteolysis residues. **(C)** HEK-293T cells in 24-well plates were transfected with PDCoV nsp5 expression plasmid or its protease-defective mutants C144A and H41A to analyze ISRE promoter activity, as described in Fig. 1B.

**FIG 3. PDCoV nsp5 inhibits type I IFN signaling by targeting STAT2. (A)** PDCoV nsp5 does not affect JAK1 and TYK2 phosphorylation and expression. PK-15 cells were transfected with PDCoV nsp5 expression plasmid or vector. After 24 h, cells were treated with IFN-α (1,000 U/ml) for 1 h and collected for western blot analysis. JAK1 antibody, TYK2 antibody, Phospho-JAK1 (P-JAK1) antibody and Phospho-TYK2 (P-TYK2) antibody were utilized to detect each respective endogenous protein. **(B)** The level of endogenous STAT2 and phosphorylation were both reduced under the expression of PDCoV nsp5. PK-15 cells were transfected with PDCoV nsp5 expression plasmid or vector and treated as described in panel A. STAT1 polyclonal antibody, STAT2 antibody, Phospho-STAT1 (P-STAT1) antibody, Phospho-STAT2 (P-STAT1) antibody were used for western blot. **(C)** HEK-293T cells were cotransfected with Flag-appended JAK1, TYK2, STAT1, STAT2, or IRF9 expression plasmids along with PDCoV nsp5. Cells were lysed at 32 h after transfection and analyzed by western blotting.

**FIG 4. PDCoV nsp5 cleaves STAT2 to disrupt type I IFN signaling. (A)**

JVI

HEK-293T cells were cotransfected with various concentrations of PDCoV nsp5 expression plasmid and Flag-appended STAT2. Cells were then lysed for western blot analysis at 32 h after transfection. **(B)** HEK-293T cells were cotransfected with wild-type PDCoV nsp5 or its protease-defective mutants (C144A and H41A) and STAT2 expression plasmid as described in panel A. **(C)** HEK-293T cells were cotransfected with wild-type PDCoV nsp5 and STAT2 expression plasmids. After 16 h, cells were treated with MG132 or Z-VAD-FMK (final concentration of 20 μM) for 8 h. Cell lysates were prepared and analyzed by western blotting. **(D)** LLC-PK1 cells were infected with PDCoV strain CHN-HN-2014 (MOI=2) and then harvested for STAT2 mRNA detection by qPCR at 18 h post-infection. **(E)** LLC-PK1 cells were infected with PDCoV as described in panel D and then lysed for western blot analysis at 18 h post-infection.

**FIG 5. Q685 and Q758 are the sites of PDCoV nsp5-mediated STAT2 cleavage.** **(A)** Sequence logo of the polyprotein junctions cleaved by PDCoV nsp5. An amino acid sequence logo of the substrate was generated by WebLogo 3 (http://weblogo.threeplusone.com/). **(B)** The estimated STAT2 cleavage product by PDCoV nsp5. HEK-293T cells were transfected with STAT2 (1–637 aa), STAT2 (1–719 aa), or STAT2 (1–758 aa) deletion mutant. Cells were then harvested and analyzed by western blot analysis. **(C)** Schematic representation of STAT2 and its mutants. **(D)** HEK-293T cells were transfected with PDCoV nsp5 and wild-type STAT2 or STAT2 mutants as indicated. Cells were lysed at 32 h after transfection and

analyzed by western blotting. **(E)** HEK-293T cells were transfected with PDCoV nsp5 and wild-type STAT2 or mutant STAT2-Q685A-Q758A as described in panel D.

**FIG 6. PDCoV nsp5-mediated STAT2 cleavage is involved in inhibition of type I IFN signaling. (A)** PK-15 cells were cotransfected with STAT1, IRF9, and wild-type STAT2 or the indicated deletion mutants, along with ISRE-Luc plasmid and pRL-TK plasmid. After 32 h, cells were harvested for luciferase assays. **(B, C and D)** PK-15 cells were transfected with expression plasmids of STAT1, STAT2, and IRF9 as described in panel A. After 32 h, cells were harvested and the mRNA levels of *ISG15* (B), *ISG54* (C) and *OAS1* (D) were detected by qPCR.

**FIG 7.** Homologous modeling of PDCoV nsp5 with the two cleaved peptide substrates. **(A and B)** Homology model of PDCoV nsp5 in complex with the cleaved peptide substrates (STAT2) based on the structure of PEDV nsp5 (PDB identifier 4ZUH). The residues EKANLQ$_{685}$ERKKYL (A) or LEPMLQ$_{758}$STLEPV (B) (P6 to P6′; numbering based on STAT2) occupy, and thereby define, the subsites S6 to S6′ of PDCoV nsp5. The positions of P6 to P6′ and potential residues forming S1′ (red) subsites are labeled. **(C and D)** The distribution of hydrophobic and hydrophilic interactions between PDCoV nsp5 and EKANLQ$_{685}$ERKKYL (C) or LEPMLQ$_{758}$STLEPV (D). Carbon, nitrogen, and oxygen atoms are marked as black, blue, and red circles, respectively. Hydrogen bonds are shown as green dashed lines labeled with the distance between the donor and corresponding acceptor atom. Arcs

JVI Journal of Virology

with spokes radiating off the atoms (spokes around) and residues (arcs with spokes) represent hydrophobic interactions.

**Table 1. Primers used for qPCR**

| Primer | Sequences (5' to 3') |
|---|---|
| h-ISG15-F | GGGACCTGACGGTGAAGATG |
| h-ISG15-R | CGCCGATCTTCTGGGTGAT |
| h-ISG54-F | CACCTCTGGACTGGCAATAGC |
| h-ISG54-R | GTCAGGATTCAGCCGAATGG |
| h-ISG56-F | GCTTTCAAATCCCTTCCGCTAT |
| h-ISG56-R | GCCTTGGCCCGTTCATAAT |
| h-OAS1-F | CGTGTTTCCGCATGCAAATC |
| h-OAS1-F | GCGAACTCAGTACGAAGCTG |
| h-GAPDH-F | TCATGACCACAGTCCATGCC |
| h-GAPDH-R | GGATGACCTTGCCCACAGCC |
| h-β-actin-F | CCTGGCACCCAGCACAAT |
| h-β-actin-R | GCTGATCCACATCTGCTGGAA |
| P-STAT2-F | TGGATGGAGAGTTGGAGCAG |
| P-STAT2-R | CTTGCTCCCAGTCTTGAGGA |
| p-ISG15-F | CCTGTTGATGGTGCAAAGCT |
| p-ISG15-R | TGCACATAGGCTTGAGGTCA |
| p-ISG54-F | CTGGCAAAGAGCCCTAAGGA |
| p-ISG54-R | CTCAGAGGGTCAATGGAATTCC |
| p-OAS1-F | AAGCATCAGAAGCTTTGCATCTT |
| p-OAS1-R | CAGGCCTGGGTTTCTTGAGTT |
| p-GAPDH-F | ACATGGCCTCCAAGGAGTAAGA |
| p-GAPDH-R | GATCGAGTTGGGGCTGTGACT |

JVI

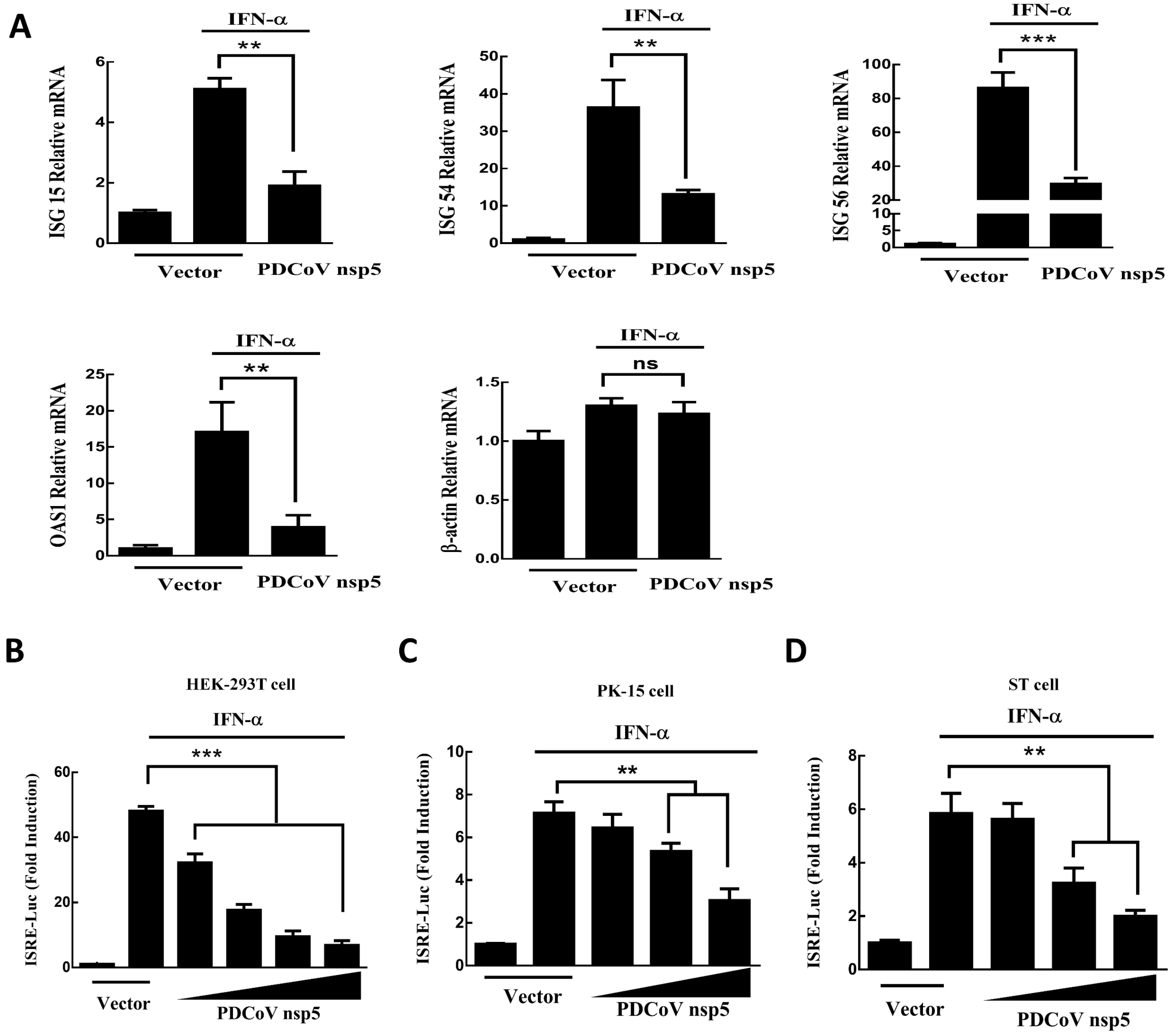
A
IFN-α
**
ISG 15 Relative mRNA
0
2
4
6
Vector
PDCoV nsp5
IFN-α
**
ISG 54 Relative mRNA
0
10
20
30
40
50
Vector
PDCoV nsp5
IFN-α
***
ISG 56 Relative mRNA
0
5
10
20
40
60
80
100
Vector
PDCoV nsp5
IFN-α
**
OAS1 Relative mRNA
0
5
10
15
20
25
Vector
PDCoV nsp5
IFN-α
ns
β-actin Relative mRNA
0.0
0.5
1.0
1.5
Vector
PDCoV nsp5
B
HEK-293T cell
IFN-α
***
ISRE-Luc (Fold Induction)
0
20
40
60
Vector
PDCoV nsp5
C
PK-15 cell
IFN-α
**
ISRE-Luc (Fold Induction)
0
2
4
6
8
10
Vector
PDCoV nsp5
D
ST cell
IFN-α
**
ISRE-Luc (Fold Induction)
0
2
4
6
8
Vector
PDCoV nsp5

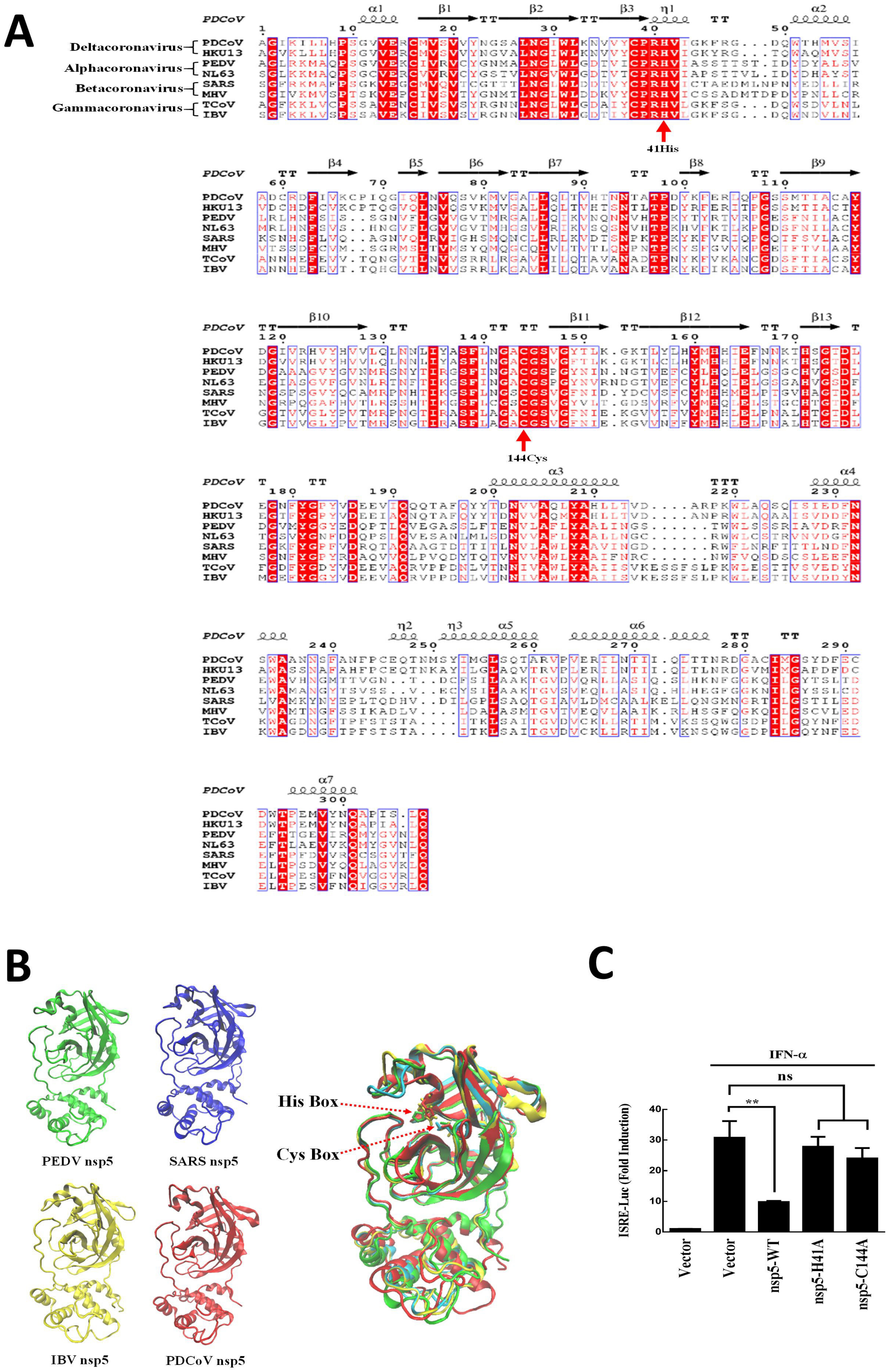
A
Deltacoronavirus
Alphacoronavirus
Betacoronavirus
Gammacoronavirus
PDCoV
HKU13
PEDV
NL63
SARS
MHV
TCoV
IBV
41His
144Cys
B
PEDV nsp5
SARS nsp5
IBV nsp5
PDCoV nsp5
His Box
Cys Box
C
IFN-α
ns
**
ISRE-Luc (Fold Induction)
40
30
20
10
0
Vector
Vector
nsp5-WT
nsp5-H41A
nsp5-C144A

JVI

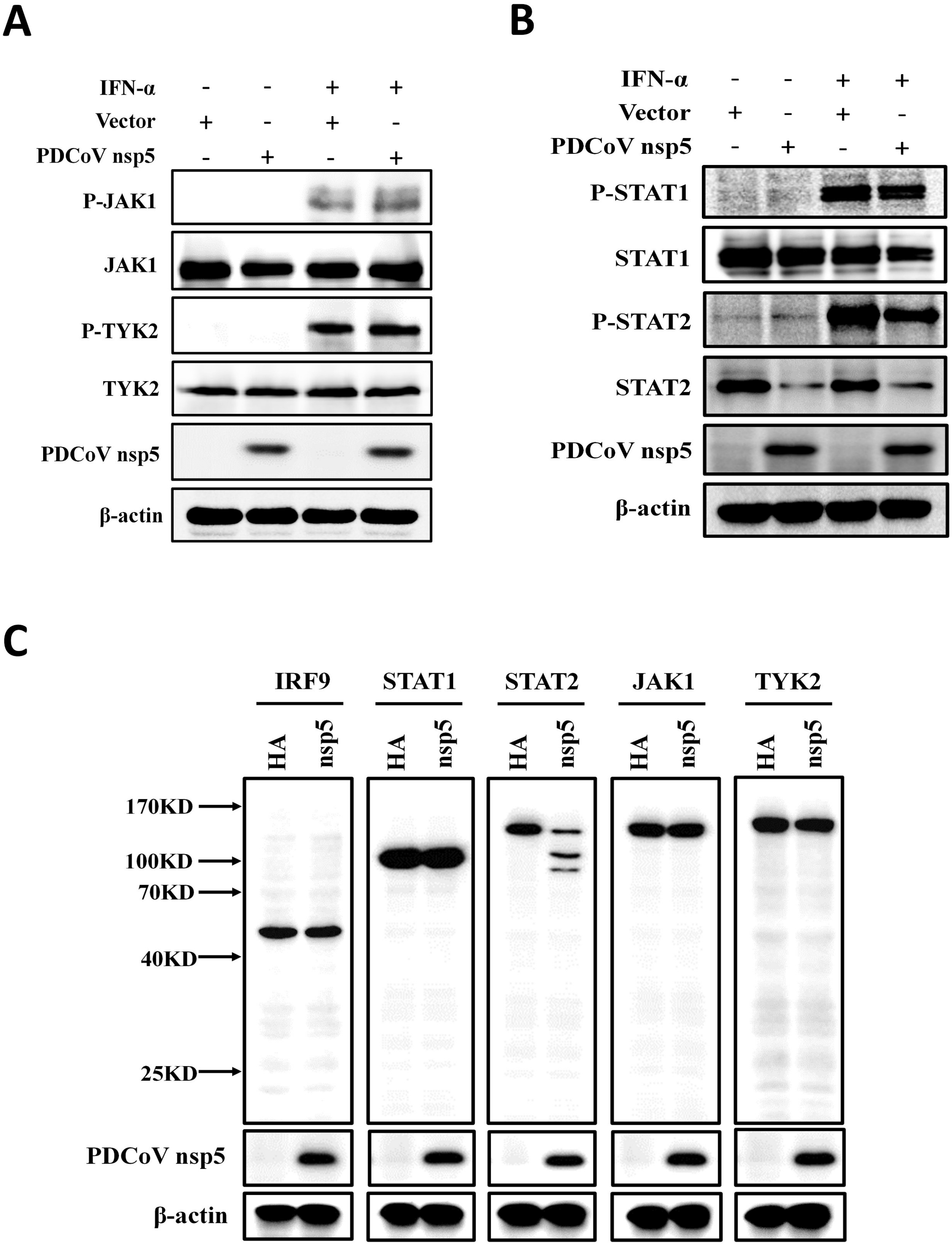
A
IFN-α - - + +
Vector + - + -
PDCoV nsp5 - + - +
P-JAK1
JAK1
P-TYK2
TYK2
PDCoV nsp5
β-actin
B
IFN-α - - + +
Vector + - + -
PDCoV nsp5 - + - +
P-STAT1
STAT1
P-STAT2
STAT2
PDCoV nsp5
β-actin
C
IRF9
STAT1
STAT2
JAK1
TYK2
HA nsp5
HA nsp5
HA nsp5
HA nsp5
HA nsp5
170KD
100KD
70KD
40KD
25KD
PDCoV nsp5
β-actin

JVI

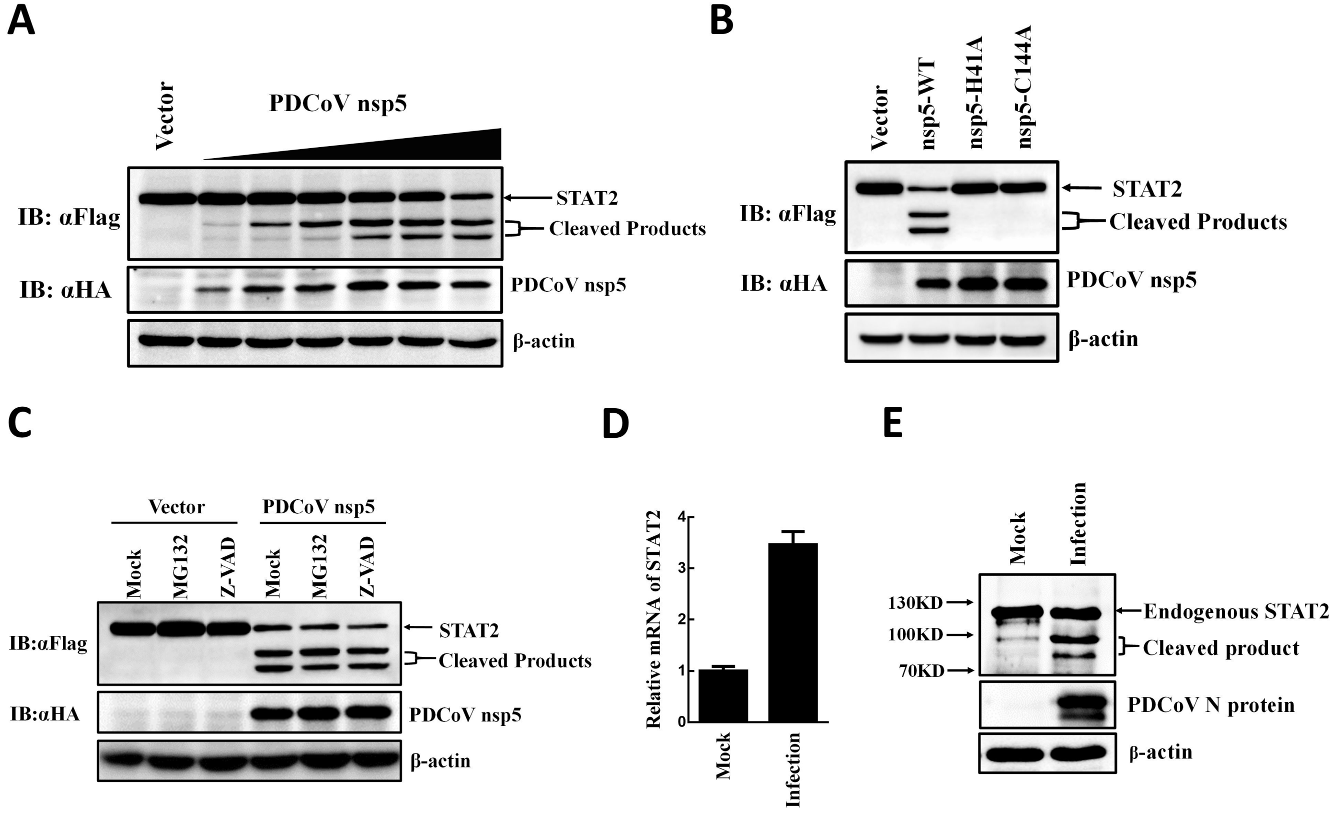
A
Vector
PDCoV nsp5
IB: αFlag
STAT2
Cleaved Products
IB: αHA
PDCoV nsp5
β-actin
B
Vector
nsp5-WT
nsp5-H41A
nsp5-C144A
IB: αFlag
STAT2
Cleaved Products
IB: αHA
PDCoV nsp5
β-actin
C
Vector
PDCoV nsp5
Mock
MG132
Z-VAD
Mock
MG132
Z-VAD
IB:αFlag
STAT2
Cleaved Products
IB:αHA
PDCoV nsp5
β-actin
D
Relative mRNA of STAT2
0
1
2
3
4
Mock
Infection
E
Mock
Infection
130KD
100KD
70KD
Endogenous STAT2
Cleaved product
PDCoV N protein
β-actin

JVI

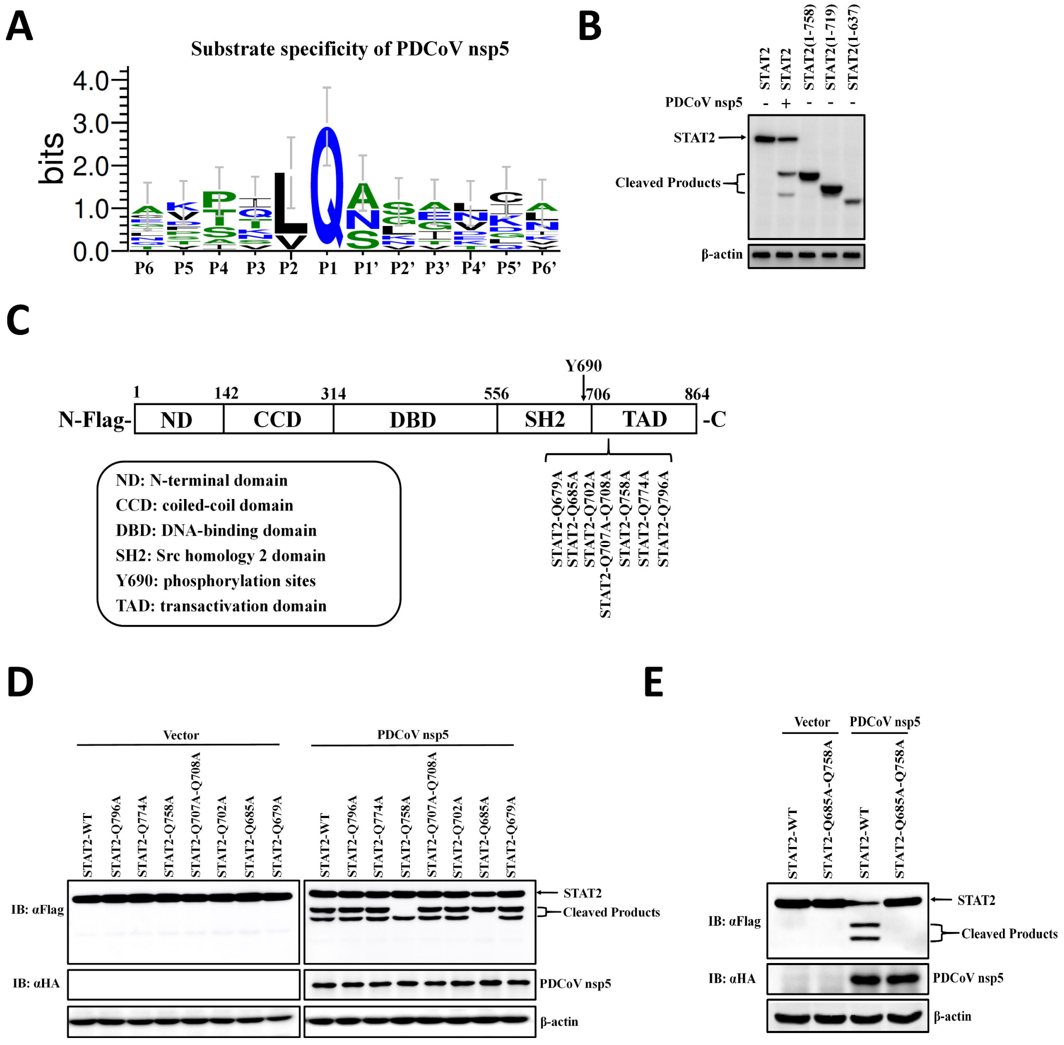
A
Substrate specificity of PDCoV nsp5
bits
4.0
3.0
2.0
1.0
0.0
P6
P5
P4
P3
P2
P1
P1'
P2'
P3'
P4'
P5'
P6'
B
STAT2
STAT2
STAT2(1-758)
STAT2(1-719)
STAT2(1-637)
PDCoV nsp5
-
+
-
-
-
STAT2
Cleaved Products
β-actin
C
Y690
1
142
314
556
706
864
N-Flag-
ND
CCD
DBD
SH2
TAD
-C
ND: N-terminal domain
CCD: coiled-coil domain
DBD: DNA-binding domain
SH2: Src homology 2 domain
Y690: phosphorylation sites
TAD: transactivation domain
STAT2-Q679A
STAT2-Q685A
STAT2-Q702A
STAT2-Q707A-Q708A
STAT2-Q758A
STAT2-Q774A
STAT2-Q796A
D
Vector
PDCoV nsp5
STAT2-WT
STAT2-Q796A
STAT2-Q774A
STAT2-Q758A
STAT2-Q707A-Q708A
STAT2-Q702A
STAT2-Q685A
STAT2-Q679A
IB: αFlag
IB: αHA
STAT2
Cleaved Products
PDCoV nsp5
β-actin
E
Vector
PDCoV nsp5
STAT2-WT
STAT2-Q685A-Q758A
STAT2-WT
STAT2-Q685A-Q758A
IB: αFlag
IB: αHA
STAT2
Cleaved Products
PDCoV nsp5
β-actin

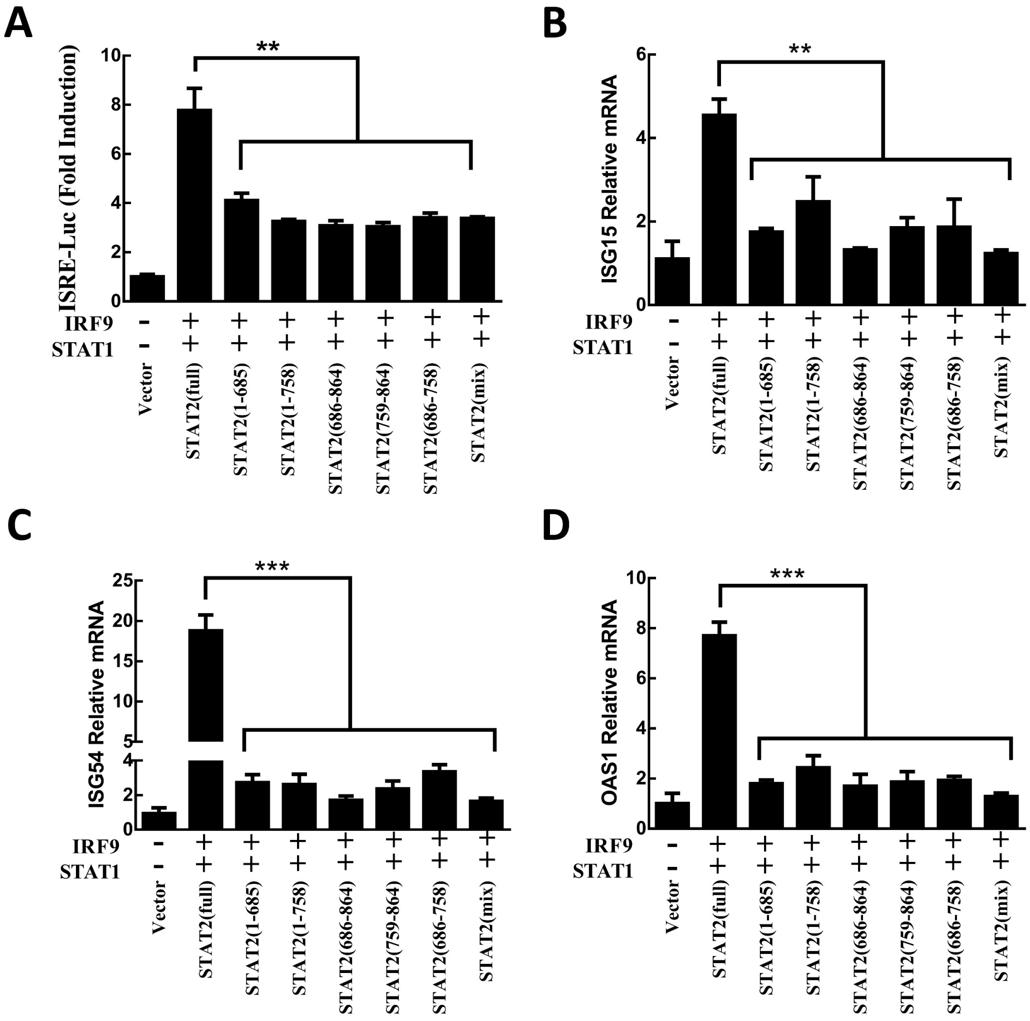
A
ISRE-Luc (Fold Induction)
0
2
4
6
8
10
**
B
ISG15 Relative mRNA
0
2
4
6
**
C
ISG54 Relative mRNA
0
2
4
5
10
15
20
25
***
D
OAS1 Relative mRNA
0
2
4
6
8
10
***
IRF9
STAT1
Vector
STAT2(full)
STAT2(1-685)
STAT2(1-758)
STAT2(686-864)
STAT2(759-864)
STAT2(686-758)
STAT2(mix)

JVI

**A**

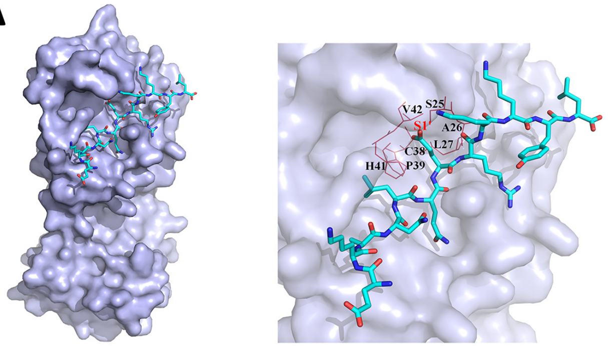

**PDCoV nsp5 in complex with**
**EKANLQ(685)↓ERKKYL**

**B**

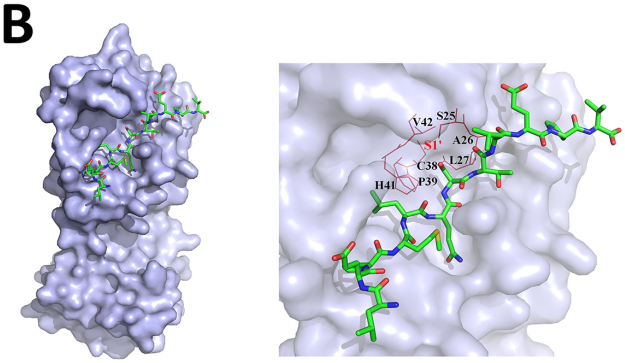

**PDCoV nsp5 in complex with**
**LEPMLQ(758)↓STLEPV**

**C**

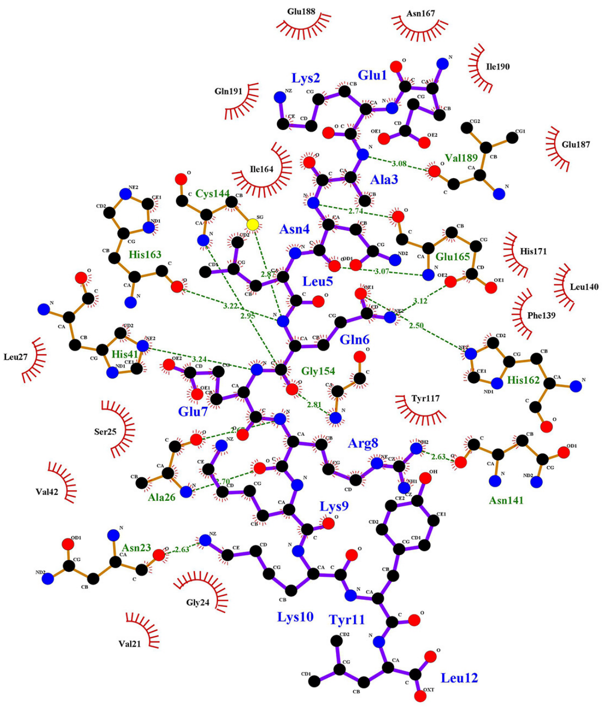

**Substrate:Glu1(P6)-Lys2(P5)-Aln3(P4)-Asn4(P3)-Leu5(P2)-Gln6(P1)(685)-Glu7(P1')-Arg8(P2')-Lys9(P3')-Lys10(P4')-Try11(P5')-Leu12(P6')**

**D**

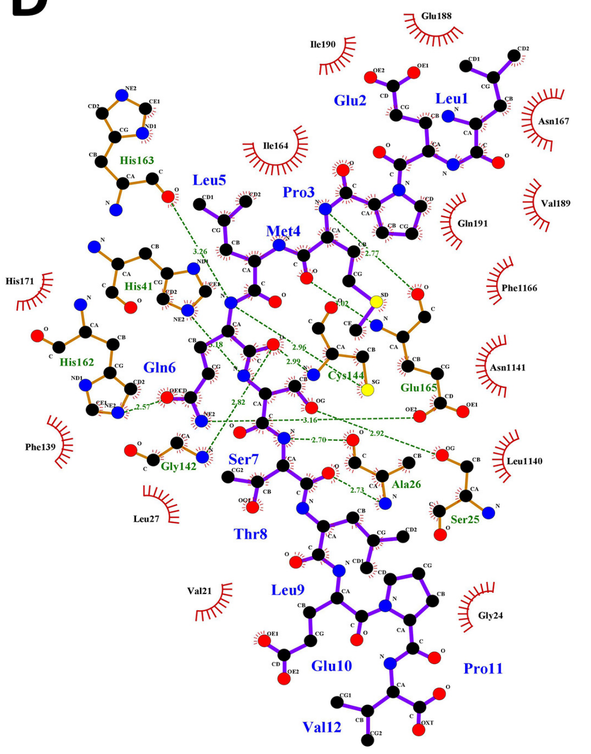

**Substrate:Leu1(P6)-Glu2(P5)-Pro3(P4)-Met4(P3)-Leu5(P2)-Gln6(P1)(758)-Ser7(P1')-Thr8(P2')-Leu9(P3')-Glu10(P4')-Pro11(P5')-Val12(P6')**